

Highly resolved data set on different phytoplankton pigments retrieved from underway spectrophotometry in the Fram Strait, Arctic Ocean

Yangyang Liu^{1,2,*}, Emmanuel Boss⁴, Alison Chase⁴, Yanqun Pan⁵, Hongyan Xi¹, Eva-Maria Nöthig¹, Sonja Wiegmann¹, and Astrid Bracher^{1,3}

¹Alfred Wegener Institute Helmholtz Centre for Polar and Marine Research, Bremerhaven, Germany

²Institute of Biology and Chemistry, University of Bremen, Bremen Germany

³Institute of Environmental Physics (IUP), University of Bremen, Bremen, Germany

⁴University of Maine, Orono, ME, USA

⁵State Key Laboratory of Estuarine and Coastal Research, East China Normal University, Shanghai, China

Introduction

- Light absorption properties of marine phytoplankton influence the solar radiation into the ocean and control the light energy usable for photosynthesis.
- The shape and magnitude of the phytoplankton absorption spectra is controlled primarily by the concentration of various pigments and the level of package effect within the cells.
- In this study, four approaches to estimate phytoplankton pigment concentration from particulate absorption spectra derived from underway AC-S flow-through system, namely **Gaussian decomposition**, **singular value decomposition**, **neural network** and **empirical orthogonal function analyses**, are evaluated and intercompared.

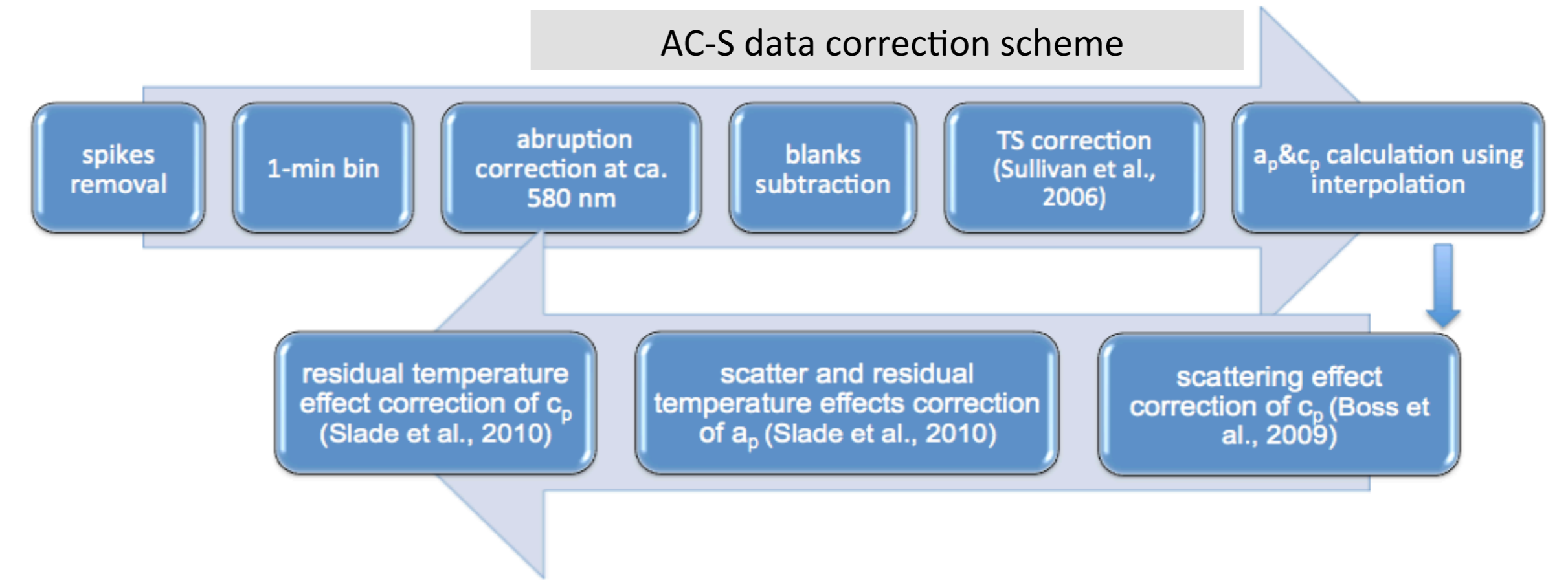
Data and Method

Cruises tracks with R.V. Polarstern

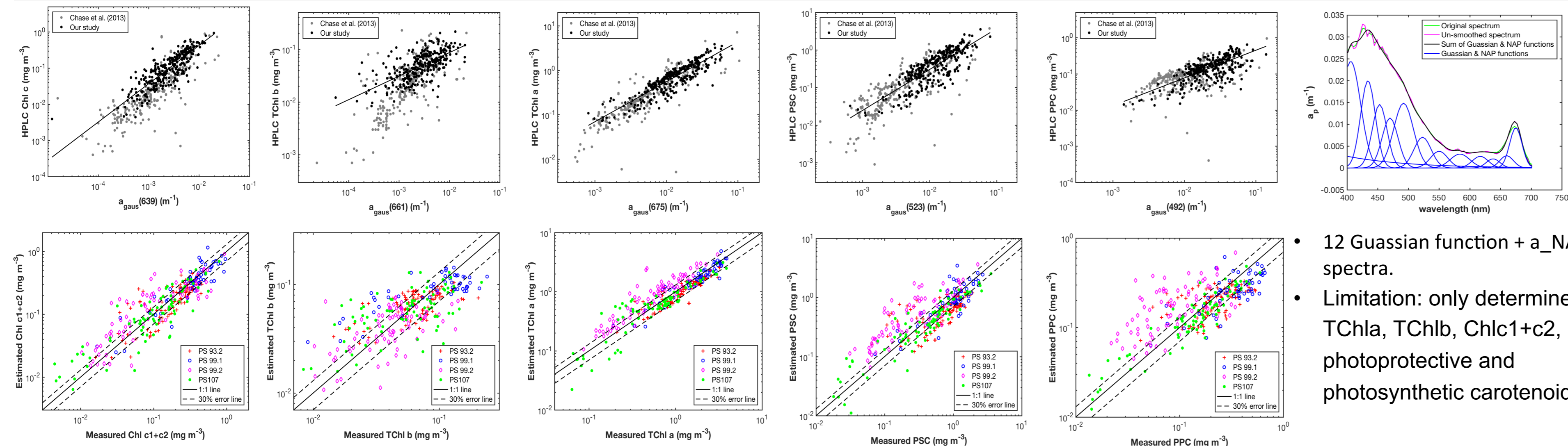
PS 93.2: Jul.-Aug. 2015, Svalbard – Fram Strait
PS 99.2: Jun.-Jul. 2016, Svalbard – Fram Strait
PS 107: Jun.-Jul. 2017, Svalbard – Fram Strait

Data

- Discrete water sampling every 3h
 - PS 93.2: a_p & a_{ph} (high performance spectrophotometer), Chl-a (HPLC)
 - PS 99.2 & PS107: a_p & a_{ph} (QFT-ICAM), Chl-a (HPLC)
- Underway AC-S measurements
 - Particulate absorption spectra



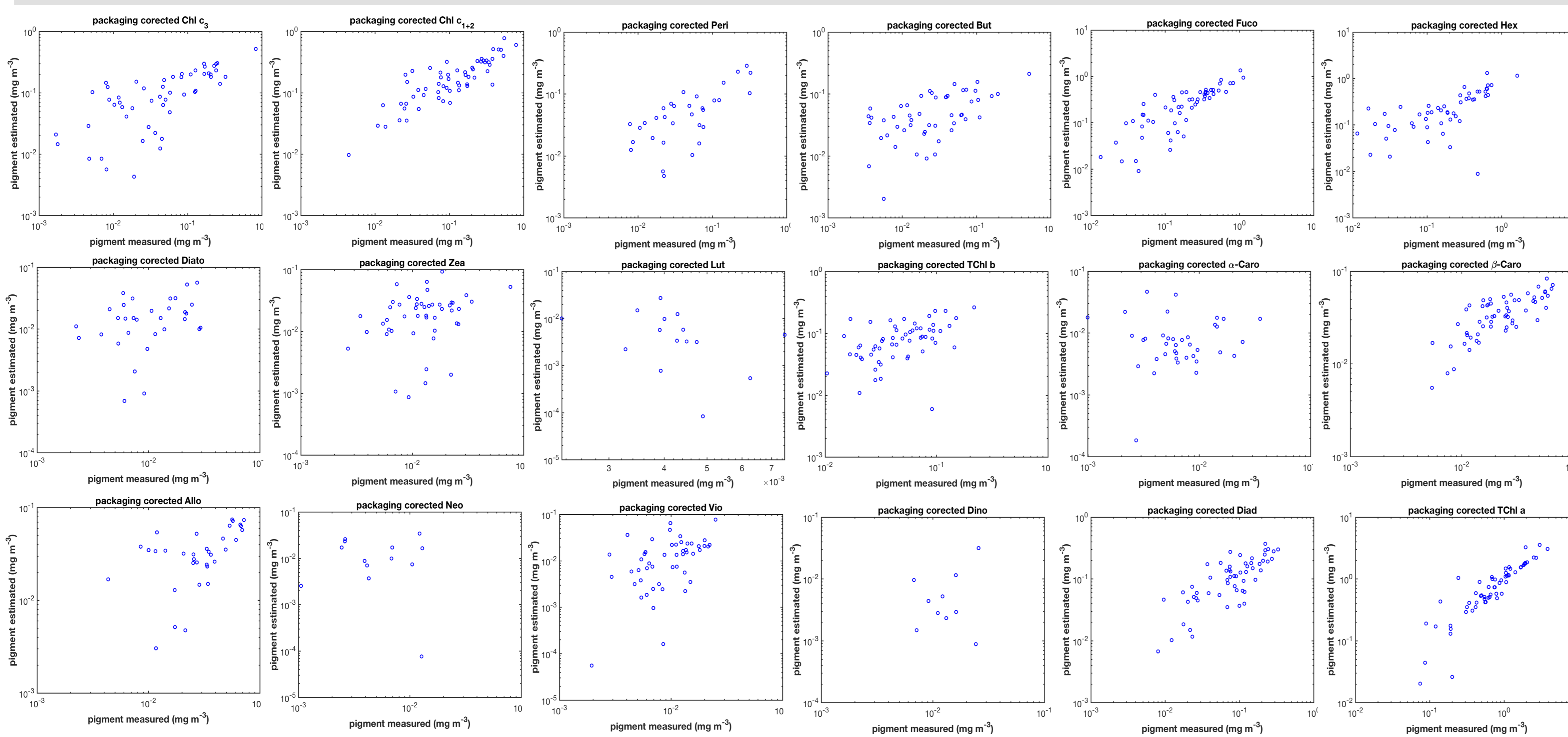
Gaussian Decomposition



- 12 Gaussian function + a_{NAP} spectra.
- Limitation: only determines TChl_a, TChl_b, Chlc_{1+c2}, photoprotective and photosynthetic carotenoids.

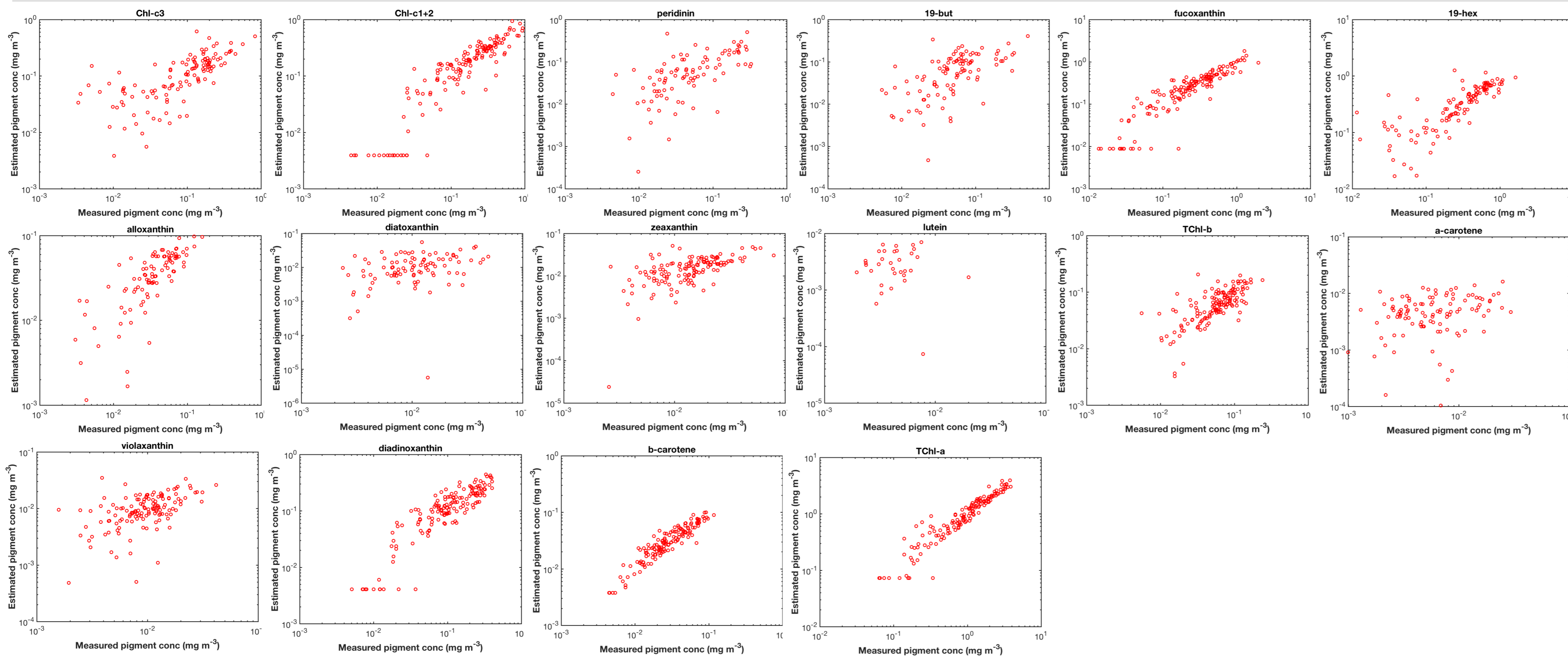
| Statistics for Gaussian Decomposition | | | | | | |
|---------------------------------------|-----------|------------|------------------|--------------|-------------|--------------|
| Pigments | <i>S</i> | <i>I</i> | <i>r</i> (log10) | RMSE (log10) | MAE (log10) | Bias (log10) |
| TChl a | 1.20±0.04 | -0.14±0.04 | 0.89 | 0.161 | 0.132 | 0.011 |
| TChl b | 2.25±0.17 | -0.06±0.01 | 0.65 | 0.201 | 0.156 | -0.001 |
| Chlc ₁₊₂ | 1.28±0.05 | -0.02±0.01 | 0.84 | 0.258 | 0.200 | 0.005 |
| PSC | 1.37±0.06 | -0.13±0.04 | 0.81 | 0.265 | 0.216 | 0.016 |
| PPC | 1.73±0.13 | -0.11±0.02 | 0.68 | 0.238 | 0.186 | 0.022 |

Singular Value Decomposition + Non-Negative Least Square



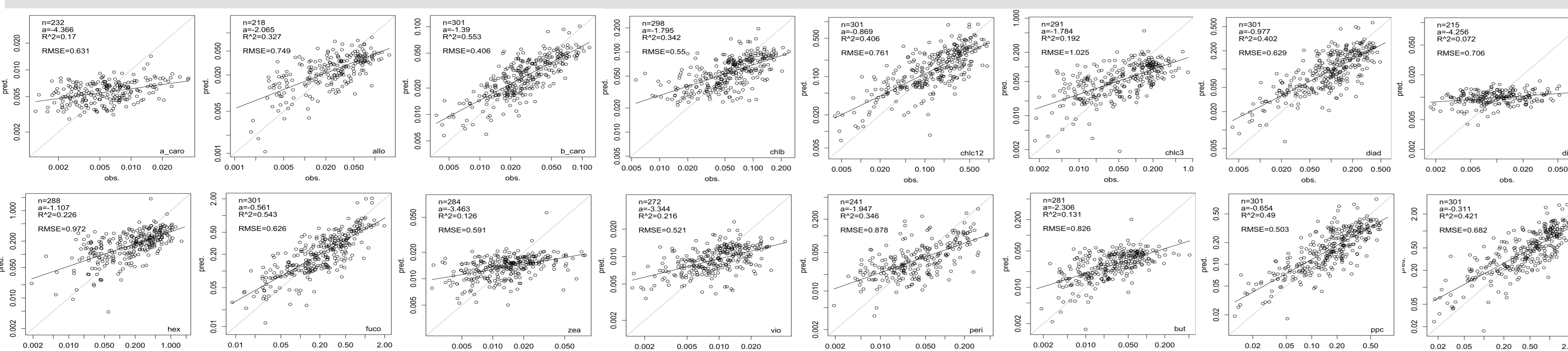
| Statistics for SVD-NNLS | | | | | | |
|-------------------------|------------|------------|------------------|--------------|-------------|--------------|
| Pigments | <i>S</i> | <i>I</i> | <i>r</i> (log10) | RMSE (log10) | MAE (log10) | Bias (log10) |
| TChl a | 0.99±0.05 | 0.03±0.06 | 0.89 | 1.243 | 1.141 | -1.141 |
| TChl b | 1.82±0.34 | -0.02±0.02 | 0.46 | 1.444 | 1.420 | -1.420 |
| Chlc ₁₊₂ | 0.91±0.07 | 0.05±0.02 | 0.85 | 1.260 | 1.199 | -1.198 |
| Chl _{c3} | 0.72±0.06 | 0.06±0.01 | 0.69 | 1.601 | 1.505 | -1.505 |
| Peri | 0.71±0.08 | 0.01±0.01 | 0.67 | 1.490 | 1.432 | -1.432 |
| But | 0.44±0.07 | 0.04±0.01 | 0.55 | 1.745 | 1.678 | -1.678 |
| Fuco | 1.07±0.07 | 0.03±0.02 | 0.81 | 1.128 | 1.091 | -1.091 |
| Hex | 0.93±0.09 | 0.03±0.03 | 0.63 | 1.147 | 1.082 | -1.082 |
| Vio | 5.43±1.48 | -0.04±0.02 | 0.50 | 2.076 | 2.062 | -2.062 |
| Diad | 1.13±0.12 | 0.01±0.02 | 0.78 | 1.304 | 1.258 | -1.258 |
| Allo | 1.03±0.18 | 0.00±0.01 | 0.49 | 1.616 | 1.591 | -1.591 |
| Diato | 3.00±1.26 | -0.02±0.02 | 0.32 | 2.044 | 2.022 | -2.022 |
| Zea | 3.02±1.32 | -0.02±0.02 | 0.27 | 1.953 | 1.934 | -1.934 |
| Lut | -17.6±13.0 | 0.08±0.06 | -0.37 | 2.382 | 2.380 | -2.380 |
| a _{Caro} | 119±3133 | -1.00±26.4 | 0.08 | 2.218 | 2.196 | -2.196 |
| B _{Caro} | 1.02±0.11 | 0.01±0.00 | 0.78 | 1.717 | 1.697 | -1.697 |
| Neo | 26.0±97.4 | -0.15±0.62 | -0.15 | 2.336 | 2.314 | -2.314 |
| Dino | 1.87±1.01 | -0.02±0.01 | 0.15 | 1.905 | 1.896 | -1.896 |

Neural Network



| Statistics for NN | | | | | | |
|---------------------|----------|----------|------------------|--------------|-------------|--------------|
| Pigments | <i>S</i> | <i>I</i> | <i>r</i> (log10) | RMSE (log10) | MAE (log10) | Bias (log10) |
| TChl a | 0.92 | 0.06 | 0.96 | 0.248 | 0.175 | -0.003 |
| TChl b | 0.75 | 0.02 | 0.69 | 0.032 | 0.022 | 0.003 |
| Chlc ₁₊₂ | 0.95 | 0.01 | 0.90 | 0.089 | 0.055 | -0.009 |
| Chl _{c3} | 0.67 | 0.02 | 0.78 | 0.078 | 0.047 | 0.001 |
| Peri | 0.85 | 0.00 | 0.66 | 0.065 | 0.034 | 0.003 |
| But | 0.75 | 0.01 | 0.67 | 0.059 | 0.036 | 0.001 |
| Fuco | 0.97 | 0.02 | 0.90 | 0.138 | 0.078 | -0.000 |
| Hex | 0.97 | 0.00 | 0.85 | 0.163 | 0.090 | 0.003 |
| Vio | 0.55 | 0.00 | 0.57 | 0.006 | 0.004 | 0.000 |
| Diad | 0.81 | 0.03 | 0.85 | 0.055 | 0.041 | 0.006 |
| Allo | 0.76 | 0.00 | 0.85 | 0.016 | 0.010 | -0.003 |
| Diato | 0.41 | 0.00 | 0.44 | 0.010 | 0.007 | 0.001 |
| Zea | 0.62 | 0.00 | 0.62 | 0.010 | 0.007 | 0.001 |
| Lut | 0.068 | 0.00 | 0.30 | 0.003 | 0.002 | -0.000 |
| a _{Caro} | 0.27 | 0.00 | 0.45 | 0.005 | 0.004 | -0.001 |
| B _{Caro} | 0.88 | 0.00 | 0.92 | 0.009 | 0.006 | 0.001 |

Empirical Orthogonal Function



References:
 Bracher, A., Taylor, M.H., Taylor, B., Dinter, T., Röttgers, R. and Steinmetz, F., 2014. Using empirical orthogonal functions derived from remote sensing reflectance for the prediction of concentrations of phytoplankton pigments. *Ocean Science Discussions*, 11(5), pp.2073-2117.
 Bricaud, A., Claustre, H., Ras, J. and Dubelkher, K., 2004. Natural variability of phytoplanktonic absorption in oceanic waters: Influence of the size structure of algal populations. *Journal of Geophysical Research: Oceans*, 109(C11).
 Chase, A., Boss, E., Zaneveld, R., Bricaud, A., Claustre, H., Ras, J., Dall'Olmo, G. and Westberry, T.K., 2013. Decomposition of in situ particulate absorption spectra. *Methods in Oceanography*, 7, pp.110-124.
 Moisan, J.R., Moisan, T.A. and Linkswiler, M.A., 2011. An inverse modeling approach to estimating phytoplankton pigment concentrations from phytoplankton absorption spectra. *Journal of Geophysical Research: Oceans*, 116(C9).
 Röttgers, R., McKee, D., & Woźniak, S. B. (2013). Evaluation of scatter corrections for ac-9 absorption measurements in coastal waters. *Methods in Oceanography*, 7, 21-39.
 Slade, W. H., Boss, E., Dall'Olmo, G., Langner, M. R., Loftin, J., Behrenfeld, M. J., Roester, C. & Westberry, T. K. (2010). Underway and moored methods for improving accuracy in measurement of spectral particulate absorption and attenuation. *Journal of Atmospheric and Oceanic Technology*, 27(10), 1733-1746.
 Sullivan, J. M., Twardowski, M. S., Zaneveld, J. R. V., Moore, C. M., Barnard, A. H., Donaghay, P. L., & Rhoades, B. (2006). Hyperspectral temperature and salt dependencies of absorption by water and heavy water in the 400-750 nm spectral range. *Applied Optics*, 45(21), 5294-5309.
 Zaneveld, J. R. V., Kitchin, J. C., & Moore, C. C. (1994, October). Scattering error correction of reflecting-tube absorption meters. In *Ocean Optics XII* (pp. 44-55). International Society for Optics and Photonics.

Outlook

- Further consider the influence of package effect to particulate absorption spectra, to get more accurate predictions of pigment concentrations.
- Different pigment concentration data will be used as input of CHEMTAX program to derive Phytoplankton Functional Types.

